

Documentation – User's Guide

SAR, InSAR and DInSAR processing with GAMMA software:

an example for ERS-ENVISAT cross-interferometry



Version 1.0 – June 2008

Table of contents

1.	INTRODUCTION	4
2.	RAW DATA PRE-PROCESSING	6
2.1.	<i>ERS-2 dataset</i>	6
2.2.	<i>ENVISAT ASAR dataset</i>	7
3.	COMPUTATION OF DOPPLER CENTROIDS	8
4.	PROCESSING OF RAW DATA TO SLC FORMAT FOR THE ERS-2 IMAGE	9
5.	PROCESSING OF RAW DATA TO SLC FORMAT FOR THE ASAR IMAGE	11
6.	ESTIMATION OF PERPENDICULAR BASELINE.....	12
7.	PREPARATION FOR PROCESSING (SLC DATA)	12
8.	CO-REGISTRATION OF THE SLCs	13
9.	INTERFEROMETRIC PROCESSING	16
9.1.	<i>Generation of the interferogram</i>	17
9.2.	<i>Generation of (initial) differential interferogram</i>	17
9.3.	<i>Removal of residual fringes from differential interferogram using fringe rate</i>	18
9.4.	<i>Generation of coherence image</i>	20
9.5.	<i>Phase unwrapping</i>	21
9.6.	<i>First refinement of differential interferogram using baseline model</i>	22
9.7.	<i>Phase unwrapping of refined differential interferogram</i>	25
9.8.	<i>Compensation of unwrapped interferogram for residual quadratic phase</i>	26
9.8.	<i>Refinement of the differential interferogram with improved quadratic phase model</i>	27
9.9.	<i>Further possible refinements and final phase unwrapping</i>	30
9.10.	<i>Conversion of unwrapped phase to elevation</i>	31
10.	REFERENCES	32

List of acronyms

ASAR	Advanced Synthetic Aperture Radar
DEM	Digital Elevation Model
DIFF&GEO	Differential Interferometry And Geocoding Software
ENVISAT	ENVIronmental SATellite
ERS	European Remote Sensing
ESA	European Space Agency
ISP	Interferometric SAR Processor
LAT	Land Application Tools
MLI	Multi-Look Intensity
MSP	Modular SAR Processor
PRF	Pulse Repetition Frequency
SAR	Synthetic Aperture Radar
SLC	Single Look Complex
SRTM	Shuttle Radar Topography Mission

1. Introduction

This document explains a full processing sequence for SAR processing, interferometric processing and differential interferometric processing using the MSP, ISP and DIFF&GEO modules of the GAMMA Software. The objective is to include in one document the individual processing aspects (e.g. generation of SLC data, co-registration, generation of interferogram, phase unwrapping etc.) described in the User's Guides of those modules.

The full processing sequence is described with an example based on a pair of images acquired by ERS-2 and ENVISAT ASAR. Nonetheless, the processing chain is in practice valid for any interferometric combination. It should be remarked that the processing steps here presented are not supposed to be taken on a 1-to-1 basis. Each dataset has its own peculiarities which might make some of the steps unnecessary whereas other steps might need iteration and further refinement.

We use an ERS-ENVISAT interferometric pair because of a slightly higher complexity in terms of processing with respect to single-sensor interferometry. This is due to the particular configuration of this interferometric system.

ERS-ENVISAT cross-interferograms can be formed when ENVISAT ASAR is in "ERS-2-like mode", i.e. Swath 2 and VV-polarization. The 28 minutes time difference between acquisitions of SAR images by the ERS-2 SAR and the ENVISAT ASAR allows obtaining interferograms with a very short repeat-pass interval compared to all other spaceborne SAR missions. This aspect makes ERS-ENVISAT coherence and interferometric phase potentially suitable for a number of applications ranging from elevation mapping to land cover classification because of the limited temporal decorrelation. Nonetheless, only under specific orbital configurations do cross-interferograms show coherence.

For a flat surface, only at perpendicular baselines of approximately 2 kilometers can the look-angle effect on the reflectivity spectrum compensate for the 31 MHz centre frequency difference between ERS and ENVISAT. The perpendicular baseline optimal for cross-interferometry is however sensitive to the local incidence angle. In general it can be said that suitable perpendicular baselines are between 1.6 and 2.4 km. For more details see [1, 2]. Here we shall remark the importance of sign. Assuming that ERS is the master image, the perpendicular baseline must be a positive value. In other words the configuration shown in Figure 1 shall occur. If the satellites switch position the condition for a "constructive" perpendicular baseline is not maintained any longer.

Another constraint to finding coherence in an ERS-ENVISAT interferometric pair is the often non-overlapping Doppler spectra of the images acquired by the two sensors. Since 2001 ERS-2 operates in the Zero-Gyro mode, which does not guarantee the stability of the satellite's orbital attitude as in the mission requirements and leads to variations of the Doppler centroid along the orbit. The variation can be significant, up to one or more Doppler ambiguities. One Doppler ambiguity corresponds to approximately 1600 Hz, i.e. the Pulse Repetition Frequency, PRF, of the two sensors. For interferometry a certain overlap of the azimuth spectra is required. As a rule of thumb image pairs with 1/3 or less common bandwidth should be discarded.

Currently the major limitation to the development of ERS-ENVISAT cross-interferometry is however more practical than technical. The archives do not provide comprehensive information on baseline and Doppler centroids yet. This implies that it is not possible to know

beforehand whether an image pair satisfies the requirement on baseline and overlap of azimuth spectra.

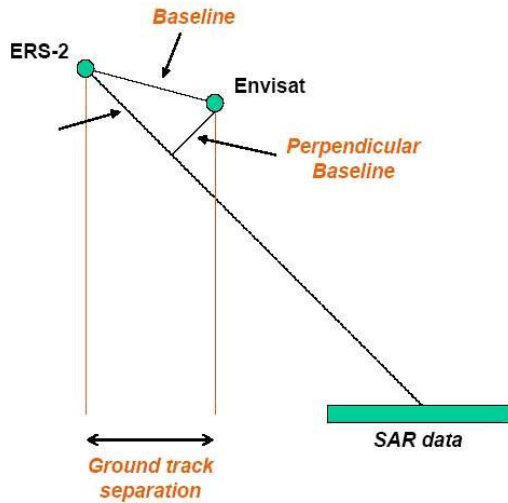


Figure 1. ERS-ENVISAT interferometric imaging geometry. ENVISAT ASAR has a 31MHz higher carrier frequency than ERS-2. The incidence angle effect compensates the carrier frequency effect on the reflectivity spectrum for a perpendicular baseline of approximately 2.0 km. The sign of the baseline is such that ENVISAT sees the area under a steeper incidence angle. ERS-2 and ENVISAT carry right looking sensors so seen in flight direction the ENVISAT orbit has to be further to the right than the ERS-2 orbit.

In this document we illustrate the processing steps and the corresponding programs required to generate an ERS-ASAR interferogram. As final result an interferometric DEM will be obtained.

For this example we use an image pair of ERS-2 and ENVISAT ASAR data acquired along track 294 on 15 October 2007 over the Seeland region, Switzerland. Data has been obtained through ESA's Cat.1 proposal 4901. The data is in raw format.

For differential interferometry we use a DEM in radar geometry. In our example this is a SRTM-3 DEM transformed to the radar geometry of the ERS-2 image using the DIFF&GEO programs for geocoding and image registration.

The processing steps described in this example consist of

- Raw data pre-processing (MSP)
- Estimation of the Doppler centroids to verify overlap of Doppler spectra (this is not needed if Doppler information is already available) (MSP)
- Perpendicular Baseline computation (ISP)
- Generation of SLC data from raw data (MSP)
- Co-registration of the ERS-2 and ENVISAT ASAR SLC datasets (ISP and DIFF&GEO)
- Generation of the interferogram, phase unwrapping and inversion to height (ISP and DIFF&GEO)

Each bullet includes a number of processing steps that will be described in the corresponding Sections. Sections 2 to 5 explain the steps to be performed to obtain SLC data from raw data. These can be neglected if the user is interested in the generation of the interferogram starting from already available SLC data. Section 6 explains how to compute the perpendicular

baseline; this is necessary if such information is not already available. The baseline length is a critical point for ERS-ENVISAT interferometry; nonetheless it should also be considered for other interferometric systems where baseline is not controlled strictly. Section 7 is designed for users starting with SLC data, explaining how to import the data for further processing with the GAMMA software. Section 8 explains the co-registration. Section 9 deals with the interferometric processing and differential interferometric processing. This is the bulk of the processing sequence presented in this document.

Part of this example can be run using the data available on the DEMO-CD ROM. For data volume reasons the set of co-registered SLC data obtained in Section 8 are provided. The dataset includes also the DEM used for differential interferometry. The SLC data can be found in the directory “slc/20071015”. The DEM can be found in the directory “dem” (file name 20071015.hgt).

2. Raw data pre-processing

The first steps consist of generating directories where the different parts of the processing will take place, convert the datasets to GAMMA format and update orbital information.

At first we generate a directory for the SAR processing called “raw” in which SAR processing will be carried out.

2.1. ERS-2 dataset

The ERS raw dataset provided by ESA consists of an image data file called DAT_01.001 and a leader file called LEA_01.001 among other files. If data are compressed, these should be first decompressed. The raw dataset and the SAR leader file shall be copied to the “raw” directory. To this directory we also copy the MSP SAR sensor parameter file and the antenna pattern file for ERS-2. These are available in the “sensors” directory which is part of the MSP directory. Assuming that the path to the MSP directory is stored in the variable \$MSP_HOME, the command lines to copy the two files are the following:

```
cp $MSP_HOME/sensors/ERS2_ESA.par .
cp $MSP_HOME/sensors/ERS2_antenna.gain .
```

We assume here that we are in the “raw” directory. The output path shall be adapted in case it differs from the example.

For ERS-2 data we need to generate the MSP SAR Processing parameter file and condition the data. The first step is done with the program ***ERS_proc_ESA***. As scene identifier we use the acquisition data (20071015).

```
ERS_proc_ESA LEA_01.001 p20071015.slc.par
```

We then convert the dataset to GAMMA format with ***ERS_fix***:

```
ERS_fix "ESA/ESRIN" ERS2_ESA.par p20071015.slc.par 0 DAT_01.001
20071015.fix
```

We also update the orbital information, for example using DELFT orbits. The update is performed with the program **DELFT_proc2**. For more details on the use of DELFT orbits for SAR processing, it is referred to the MSP User's Guide. It is recommended to store the orbital data in a directory. In this example the directory containing the orbit files (called ODR*) is called /home/Delft_orbits/ers2/dgm-e04.

```
DELFT_proc2 p20071015.slc.par /home/Delft_orbits/ers2/dgm-e04 9 10
```

At the time of creating this example the ODR file for the acquisition date were not available. Hence the orbits have not been updated.

2.2. ENVISAT ASAR dataset

ENVISAT ASAR data are delivered as one file containing image and metadata. We therefore need to convert the data to GAMMA format, i.e. generate an image data file and the MSP SAR sensor and processing parameter files.

We assume that we are in the “raw” directory. The path shall be adapted in case it differs from the example.

At first we proceed with the generation of the antenna pattern file for the specific acquisition geometry (IS2, VV polarization) using the program **ASAR_XCA**. For this an external calibration file provided by ESA (ASA_XCA*) is required. In this example we use the file ASA_XCA_AXVIEC20060717_154125_20050916_195733_20061231_000000. This can be copied to the processing directory. For the antenna pattern file we have chosen the file name “antenna_gain”

```
ASAR_XCA      ASA_XCA_AXVIEC20060717_154125_20050916_195733_20061231_000000
antenna_gain IS2 VV
```

The raw dataset is reformatted to the GAMMA Software format with the program **ASAR_IM_proc**. The MSP processing parameter file and the SAR processing parameter file are also produced. The original ASAR file is called. ASA_IM__OCNPDK20071015_095156_000000172062_00294_29406_4228.N1. This file shall be copied to the working directory if not already done.

```
ASAR_IM_proc ASA_IM__OCNPDK20071015_095156_000000172062_00294_29406_4228.N1
ASA_INS_AXVIEC20051219_161945_20030211_000000_20061231_000000
ASAR.IS2.VV.par pA20071015.slc.par A20071015.fix antenna_gain
```

For processing the ASAR instrument characterization file is required. This file is provided by ESA. For this example we use the file ASA_INS_AXVIEC20051219_161945_20030211_000000_20061231_000000. The output consists of the MSP sensor parameter file ASAR.IS2.VV.par, the MSP processing parameter file and the corresponding image file. For these the file name A20071015 has been used, to distinguish it from the ERS image acquired on the same day.

Finally we improve the orbital information. Here we use the DORIS orbits as follows:

```
DORIS_proc pA20071015.slc.par doris_file 9
```

With doris_file we indicate the file with the DORIS orbits covering the date of acquisition. This can be identified by comparing the date of the image with the dates covered by each

specific DORIS orbits file. For more details on the use of DORIS orbits for SAR processing, it is referred to the MSP User's Guide. It is recommended to store all orbits in a directory to facilitate access to a specific date.

At the time when this example was created the DORIS orbits for the acquisition date were not available yet. Hence the orbits have not been updated.

If the orbits are not available (e.g. the acquisition data is very recent) we can propagate the orbital information provided by ESA with the program ***ORB_prop*** as follows

```
ORB_prop pA20071015.slc.par 9 10 30
```

Here we generate 9 state vectors with 10 seconds interval and with 30 seconds extra information at the beginning and end of the image dataset.

3. Computation of Doppler Centroids

The overlap of the Doppler spectra is a major requirement for ERS-ENVISAT cross-interferometry to be meaningful. If this information is not available in ESA's catalogues, Doppler information can be estimated from the raw data. In theory it is necessary to computer the Doppler spectrum only for the ERS-2 image since ENVISAT ASAR data have a quite rather stable Doppler Centroid of around 200-300 Hz.

For single-sensor interferometry the Doppler spectra overlap is less relevant since in most cases the Doppler is similar. Only ERS-2 after 2000 presented large variations of the Doppler Centroid that limit the application of interferometry.

Estimation of the Doppler spectrum for ERS-2 requires that raw data are converted to the GAMMA Software format first. The steps required to estimate the Doppler spectra have been described in the User's Guide of the MSP module. For this reason only the processing steps will be presented. For more information on the specific processing steps it is referred to the MSP User's Guide.

To estimate the Doppler spectrum we use the program ***azsp_IQ*** as follows. It is assumed we are in the "raw" directory.

```
azsp_IQ ERS2_ESA.par p20071015.slc.par 20071015.fix 20071015.azsp -- 12 1
```

The Doppler estimate is equal to -32.78 Hz. This however is an ambiguous estimate in the sense that the PRF estimated by ***azsp_IQ*** does not account for multiples of the PRF. To resolve the ambiguity one of the programs ***dop_ambig*** or ***dop_mlcc*** can be run. For details see the User's Guide of the MSP. To further confirm the unambiguity of the estimate of the Doppler centroid the program ***autof*** can be run. In our example we don't have ambiguities.

The Doppler spectrum for the ENVISAT ASAR dataset can then be obtained simply with the program ***azsp_IQ*** since the Doppler centroid of ENVISAT is stable and withing the \pm PRF/2 interval.

```
azsp_IQ ASAR.IS2.VV.par pA20071015.slc.par A20071015.fix A20071015.azsp -- 12 1
```

The Doppler Centroid is 204.6 Hz. The difference of the Doppler Centroid is \sim 240 Hz, i.e. the overlap of the Doppler spectra is good.

If the Doppler Centroids are rather similar the two raw datasets could be in theory processed using the same Doppler centroid and adjusting the bandwidth to be processed in order to capture the common band. This corresponds to a sort of common-band filter in azimuth. In this way we can avoid the common-band filtering in azimuth implemented in the interferometric processing. The disadvantage in this case is that the processing becomes more manual. If the Doppler centroids are different, e.g. order of half bandwidth, i.e. 800 Hz or so, it is recommended to process the two datasets using their own Doppler centroids. In this case common-band filtering in azimuth will have to be done during interferometric processing.

The value of the Doppler Centroid can be changed either manually by opening the MSP processing parameter file with a text editor or by using the program *set_value* where the keyword "doppler_polynomial" is specified. It is recommended to create a copy of the input MSP processing parameter file beforehand. For example if we wanted to set the Doppler polynomial to a constant value equal to 200 Hz, i.e. to a value similar to the ASAR Doppler Centroid, the command line would look as follows:

```
mv p20071015.slc.par p20071015.slc.par.orig  
set_value p20071015.slc.par.orig p20071015.slc.par "doppler_polynomial"  
"2.00000e+02 0.00000e+00 0.00000e+00 0.00000e+00"
```

In this example we will process the data to the original Doppler Centroids. We could have also chosen to process to the same Doppler centroid and set the bandwidth manually since the difference between the Doppler Centroids is rather small. However we prefer to run the commands in a more automatic manner and let the program that will generate the interferogram do the common-band filtering in azimuth.

Before deciding whether the image pair is suitable for cross-interferometry, we need to estimate the perpendicular component of the baseline. If this information is not available beforehand, it can be computed from the acquisition geometry parameters and the orbital data with the ISP program *base_orbit*. This program requires the availability of the ISP SLC parameter files. For this reason, it is necessary to generate the SLC images from the raw datasets.

4. Processing of raw data to SLC format for the ERS-2 image

SAR processing has been described in the User's Guide of the MSP module. For this reason only the processing steps will be presented. For more information on the specific processing steps it is referred to the Example on ERS SAR data processing in the MSP User's Guide.

It is assumed we are in the "raw" directory. It is also assumed we have already computed the azimuth spectrum (see Section 3). If this was not done yet, it should be done before starting the processing.

Computation of range spectrum

```
rspec_IQ ERS2_ESA.par p20071015.slc.par 20071015.fix 20071015.rspec
```

Range compression

```
pre_rc ERS2_ESA.par p20071015.slc.par 20071015.fix 20071015.rc 1
```

Autofocus

```
autof ERS2_ESA.par p20071015.slc.par 20071015.rc 20071015.autof 2.0 1 4096
```

```
autof ERS2_ESA.par p20071015.slc.par 20071015.rc 20071015.autof 2.0 1 4096
```

Azimuth compression

```
az_proc ERS2_ESA.par p20071015.slc.par 20071015.rc 20071015.slc 4096 1 57.2  
0 2.120
```

Since we want the SLC to be in SCOMPLEX format, we add to the calibration factor of -2.8 dB (see the calibration table sensor_cal_MSP.dat in the \$MSP_HOME/sensors directory) a factor of 60 dB. This results in scaling the image with the factor 57.2 dB.

At this point we can generate the ISP SLC/MLI parameter files for the SLC starting from the corresponding MSP processing parameter files.

```
par_MSP ERS2_ESA.par p20071015.slc.par 20071015.slc.par
```

The output will consist of:

- SLC image 20071015.slc (width: 4912 pixels, length: 26065 pixels)
- corresponding parameter files for the MSP and the ISP modules (p20071015.slc.par and 20071015.slc.par respectively)

Figure 2 shows the magnitude of the SLC image. This can be displayed with the DISP program **disSLC** or saved to SUNraster/bmp format with the program **rasSLC**.

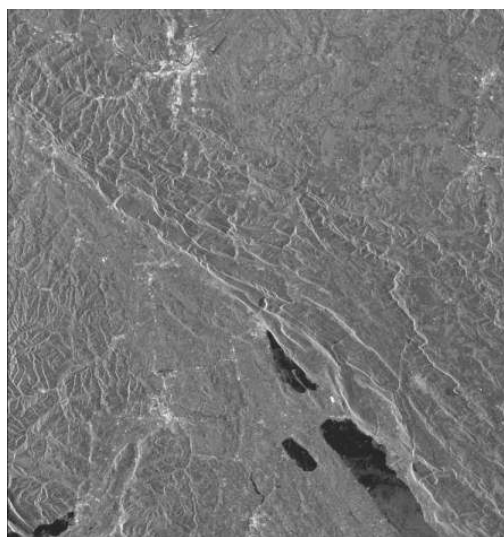


Figure 2. Magnitude of ERS-2 SAR image. The image is in radar geometry. The bright area at the top corresponds to the Berne agglomeration. At the bottom the three lakes of Biel, Neuchatel and Murten are recognizable. The Seeland region is located between the three lakes.

5. Processing of raw data to SLC format for the ASAR image

SAR processing has been described in the User's Guide of the MSP module. For this reason only the processing steps will be presented. For more information on the specific processing steps it is referred to the Example on ENVISAR ASAR data processing in the MSP User's Guide.

It is assumed we are in the "raw" directory. It is also assumed we have computed the azimuth spectrum (see Section 3). If this was not done yet, it should be done before starting the processing.

Computation of range spectrum

```
rspec_IQ ASAR.IS2.VV.par pA20071015.slc.par A20071015.fix A20071015.rspec
```

Range compression

```
pre_rc ASAR.IS2.VV.par pA20071015.slc.par A20071015.fix A20071015.rc 1
```

Autofocus

```
autof ASAR.IS2.VV.par pA20071015.slc.par A20071015.rc A20071015.autof 2.0 1  
4096
```

```
autof ASAR.IS2.VV.par pA20071015.slc.par A20071015.rc A20071015.autof 2.0 1  
4096
```

Azimuth compression

```
az_proc ASAR.IS2.VV.par pA20071015.slc.par A20071015.rc A20071015.slc 8192  
1 29.6 0
```

Since we want the SLC to be in SCOMPLEX format, we add to the calibration factor of -30.4 dB (see the calibration table sensor_cal_MSP.dat in the \$MSP_HOME/sensors directory) a factor of 60 dB. This results in scaling the image with the factor 29.6 dB.

At this point we can generate the ISP SLC/MLI parameter file for the SLC image starting from the corresponding MSP processing parameter files.

```
par_MSP ASAR.IS2.VV.par pA20071015.slc.par A20071015.slc.par
```

The output will consist of:

- SLC image A20071015.slc (width: 5182 pixels, length: 25802 pixels)
- corresponding parameter files for the MSP and the ISP modules (pA20071015.slc.par and A20071015.slc.par respectively)

Figure 3 shows the magnitude of the SLC image. This can be displayed with the DISP program *disSLC* or saved to SUNraster/bmp format with the program *rasSLC*.

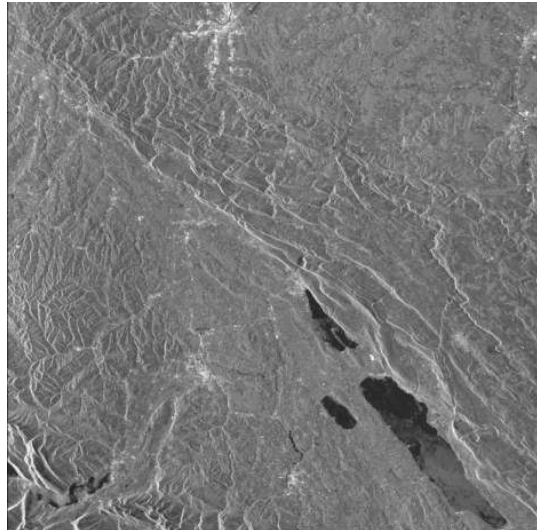


Figure 3. ENVISAT ASAR MLI image. The image is in radar geometry. With respect to Figure XX there is a large shift in azimuth (vertical direction) and a smaller shift in range (horizontal direction) due to the long baseline between ERS and ASAR.

6. Estimation of perpendicular baseline

For the computation of the perpendicular baseline we consider in the following ERS-2 to be the reference satellite. The command line looks as follows:

```
base_orbit 20071015.slc.par A20071015.slc.par 20071015_A20071015.base_orbit
```

The perpendicular component of the baseline is equal to 1899.4 m. Here we remark the importance of the sign of the baseline.

Since the requirements on both the Doppler Centroids and the perpendicular components of the baseline are met, we can proceed with the co-registration and generation of the interferogram.

It should be noted that this aspect can be relevant also for single-sensor SAR interferometry. Interferometry with ERS-2, JERS, RADARSAT-1 and ENVISAT data pairs might not be suited in some cases because of the very long baseline due to the large orbital tube of these satellites.

7. Preparation for processing (SLC data)

If the dataset for cross-interferometry consists of SLC data obtained for example from ESA the data have to be converted to GAMMA format with the program ***par_ESA_ESR*** and ***par_ASAR***. In the corresponding ISP SLC parameter files the Doppler information is contained.

In this case it is not possible to set the Doppler Centroid to a common value. It is therefore advised that image pairs presenting large Doppler differences (more than half bandwidth, i.e. 800 Hz) may result unsuitable for cross-interferometry.

To compute the perpendicular baseline the program **base_orbit** can be used as shown in Section 6. However it is recommended to improve the orbital information with one of the external sources for orbital data. For this it is referred to the ISP User's Guide. Radiometric calibration of the data can also be performed. For more details it is referred to the ISP User's Guide.

8. Co-registration of the SLCs

For the co-registration of the SLCs we use the lookup table approach. For more details it is referred to the User's Guide on Geocoding and Image Registration of the DIFF&GEO module. Besides the SLC and the corresponding MLI data, a DEM is required. It is important here to remark that this approach allows taking into account the different range and azimuth sampling, which is not the case when using the traditional cross-correlation algorithm.

Here we assume that the co-registration will be done in a directory called "coreg", at the same level as the "raw" directory. We will assume that all data required for processing are available in the directory "coreg". In this way we avoid long file names including relative paths on the command line. This means that the SLC images, the SLC parameter files as well as the DEM required for the co-registration have been copied to this directory.

In this example we will restrict the co-registration and the generation of the interferogram to a small area corresponding to the Seeland region between the three lakes. The reason is that this area is rather flat and therefore will not be affected by the geometric decorrelation due to the long baseline. All other areas are characterized by hilly topography and will be in any case affected by strong geometric decorrelation. This could cause problems when for example refining the baseline or unwrapping the interferogram (see Section 9 for more details).

To generate the subset of the reference SLC the command **SLC_copy** is applied as follows.

```
SLC_copy 20071015.slc 20071015.slc.par 20071015.rsclc 20071015.rslc.par 4  
1.0 2400 750 17500 4000
```

The subset called 20071015.rsclc will be 750 lines wide and 4000 lines long. With the command **multi_look** we then generate the corresponding MLI image (20071015.rmli) with multi look factors 1 and 5 to obtain roughly 20-m pixel size.

```
multi_look 20071015.rsclc 20071015.rslc.par 20071015.rmli 20071015.rmli.par  
1 5
```

Figure 4 illustrates the MLI image of the subset.

The co-registration will now consist of resampling the ENVISAT ASAR SLC to the geometry of the ERS-2 subset. For the co-registration we will need the MLI image of the ASAR image as well. This can be obtained with the program **multi_look** as follows. The same multi-look factors as for the ERS-2 image are used.



Figure 4. MLI image of the Seeland region. The subset is 750 pixels wide and 800 pixels long.

The MLI image will be 5182 pixels wide and 5160 pixels long

```
multi_look A20071015.slc A20071015.slc.par A20071015.mli A20071015.mli.par  
1 5
```

At first we generate the co-registration lookup table with the command ***rdc_trans*** taking into account that the ERS-2 image is the reference.

```
rdc_trans 20071015.rmlri.par 20071015.hgt A20071015.mli.par 20071015.lt0
```

To generate the lookup table we need a DEM in the geometry of the reference SAR image. In this example we assume that the DEM is already in the radar geometry and matches with the reference SAR image. The DEM in radar geometry can be obtained from a DEM in a given map projection following the procedure described in Example B in the User's Guide on Geocoding and Image Registration of the DIFF&GEO module. The DEM in radar geometry is called 20071015.hgt.

For assessing the overlap between the two MLIs the co-registration lookup table is used to convert the reference MLI image to the geometry of the other image in the program ***geocode***:

```
geocode 20071015.lt0 20071015.rmlri 750 20071015.rmlri0 5182 5160 2 0
```

Because of inaccuracies in the orbital data the two images do not match perfectly. With the DISP program ***dis2pwr*** the offsets between the co-registered MLI images can be appreciated

```
dis2pwr 20071015.rmlri0 A20071015.mli 5182 5182
```

For refining the co-registration lookup table we use the cross-correlation algorithm for two MLI images. The offsets between the transformed reference MLI (file *.rmlri0) and the MLI of the other image are determined. For this we use the sequence ***create_diff_par***, ***init_offsetm***, ***offset_pwrm***, ***offset_fitm*** as follows. The size of the windows used in ***offset_pwrm*** and their number as well as the number of terms in offset polynomial from ***offset_fitm*** refer to the specific case being considered. These figures might need to be adapted to the specific test case. It is referred to the User's Guide on Geocoding and Image Registration of the DIFF&GEO module for more information.

```
create_diff_par A20071015.mli.par - A20071015.diff0 1  
offset_pwr 20071015.rmlio A20071015.mli A20071015.diff0 A20071015.offset0  
A20071015.snr0 128 128 - 2 32 32  
offset_fitm A20071015.offset0 A20071015.snr0 A20071015.diff0 -- 7.0 4
```

The offset statistics are very good with std. deviation of the offsets below 0.04 times the MLI pixel spacing, i.e. roughly 0.8 m.

The model for the offsets can now be used to refine the lookup table with ***gc_map_fine***:

```
gc_map_fine 20071015.lt0 750 A20071015.diff0 20071015.lt1
```

The ENVISAT ASAR SLC can now be resampled to the geometry of the reference SLC with the program ***SLC_interp_lt***.

```
SLC_interp_lt      A20071015.slc      20071015.rslc.par      A20071015.slc.par  
20071015.lt1     20071015.rmlipar    A20071015.mli.par    -   A20071015.rslc0  
A20071015.rslc0.par
```

To correct for possible residual offsets we can refine the co-registration between the reference ERS-2 SLC (20071015.rslc) and the resampled ASAR SLC (A20071015.rslc0) using the cross-correlation algorithm. Details can be found in the ISP User's Guide. In this example we only report the command lines.

1) Generation of offset parameter file (all default values are accepted)

```
create_offset 20071015.rslc.par A20071015.rslc0.par 20071015_A20071015.off  
1 1 5
```

2) Offset computation and generation of offset polynomials. These figures might need to be adapted to the specific test case. It is referred to the User's Guide on Geocoding and Image Registration of the ISP module for more information.

```
offset_pwr      20071015.rslc      A20071015.rslc0      20071015.rslc.par  
A20071015.rslc0.par    20071015_A20071015.off    20071015_A20071015.offsets  
20071015_A20071015.snr 128 128 - 2 8 32  
  
offset_fit      20071015_A20071015.offsets      20071015_A20071015.snr  
20071015_A20071015.off -- 7.0 4
```

In this case the error statistics are of the order of 0.02-0.04 times the SLC pixel spacing, i.e. 0.1-0.8 m in (ground) range and azimuth.

3) New resampling of the ASAR SLC using offset information in the offset parameter file together with the lookup table.

```
SLC_interp_lt      A20071015.slc      20071015.rslc.par      A20071015.slc.par  
20071015.lt1     20071015.rmlipar    A20071015.mli.par    20071015_A20071015.off  
A20071015.rslc A20071015.rslc.par
```

4) Generation of MLI image from resampled SLC

```
multi_look      A20071015.rslc      A20071015.rslc.par      A20071015.rmlipar  
A20071015.rmlipar 1 5
```

The set of co-registered SLC and MLI images consists of

- ERS-2 (reference) SLC: 20071015.rslc and 20071015.rslc.par
- ERS-2 (reference) MLI: 20071015.rmli and 20071015.rmli.par
- ENVISAT ASAR SLC: A20071015.rslc and A20071015.rslc.par
- ENVISAT ASAR MLI: A20071015.rmli and A20071015.rmli.par

The initial version of the co-registered ASAR SLC (A20071015.rslc0) can be deleted.

Note: The co-registered SLC data *.rslc are provided on the DEMO CD-ROM, the MLI images can be obtained using the *multi_look* commands described in this Section. If the dataset is used for following the processing steps described in the next Section it is recommended to copy the SLC data to a working directory. Also the DEM in radar geometry available on the CD-ROM should be copied to this directory.

9. Interferometric processing

The objective is to generate a differential interferogram and a coherence image starting from the co-registered SLC images and the DEM in the radar geometry. From the differential interferogram we want to obtain an elevation model.

The processing steps are summarized below:

- Generation of the interferogram
- Generation of the (initial) differential interferogram
- Removal of residual fringes from the differential interferogram using the fringe rate
- Generation of the coherence image
- Phase unwrapping of the differential interferogram
- First refinement of the differential interferogram for residual baseline component using a baseline model
- Phase unwrapping of the refined differential interferogram
- Compensation for residual quadratic phase component
- Refinement of the differential interferogram with improved quadratic phase model
- Conversion of the differential interferogram to elevation

This example does not include corrections for atmospheric artifacts since there were no visible artifacts affecting the scene. We also neglect possible deformations because of the very short repeat-pass interval. Finally we assume that the DEM used for differential interferometry is good enough for the scope of this example. At the end of this document some advises are given for the case of residual phase components due to inaccuracies of the DEM.

The processing will take place in a directory called “int”, which we assume to be at the same level as the other two directories “raw” and “coreg”. For processing we need to copy the co-registered SLC and MLI images (see above) as well as the DEM in radar geometry (20071015.hgt) from the “coreg” directory to the “int” directory. If running the example with data on the DEMO-CD ROM the user’s working directory can be said to correspond to the “int” directory.

As file identifier for the interferometric products we will use the combination of the file identifiers for the two images: 20071015_A20071015. Since we will produce a large number of files all with this file identifier, we will refer with an asterisk * to it and specify the extension of the specific file for the sake of simplicity.

9.1. Generation of the interferogram

The first step is to generate an ISP offset parameter file in which the parameters describing the interferogram will be stored (*.off).

```
create_offset 20071015.rslc.par A20071015.rslc.par 20071015_A20071015.off 1
```

We then need to compute the baseline for the subset from the orbital information. The baseline estimate will be stored in a file *.base.orbit. The initial estimate obtained in Section 6 was relative to the entire scene. The baseline changes along track and precise information on it is required for cross-interferometry so that re-computation is recommended.

```
base_orbit          20071015.rslc.par          A20071015.rslc.par  
20071015_A20071015.base.orbit
```

The estimated perpendicular and parallel components of the baseline from the orbits are 1890.9651 and 598.9799 m respectively.

The computation of the interferogram is done with the program **SLC_intf** as follows

```
SLC_intf 20071015.rslc A20071015.rslc 20071015.rslc.par A20071015.rslc.par  
20071015_A20071015.off 20071015_A20071015.int 1 5
```

The interferogram is stored in the file *.int. The program applies common band filtering both in range and in azimuth. The SLC azimuth bandwidth fraction is 0.8000 whereas the filter bandwidth fraction is 0.6587. This tells us that large part of the azimuth spectrum has been used, which we could guess because of the small difference of the Doppler Centroids (see Section 3). Because of the nearly optimal baseline the range spectra present a certain offset. The common range bandwidth fraction decreases from 0.53 to 0.48 when going from near to far range. The variation across range is due to the variation of the perpendicular baseline.

9.2. Generation of (initial) differential interferogram

From the initial baseline estimate and the DEM in SAR geometry we generate a simulated phase image consisting of curved Earth and topographic fringes using the program **phase_sim**. The simulated phase image *.ph_sim is unwrapped.

```
phase_sim          20071015.rslc.par          20071015_A20071015.off  
20071015_A20071015.base.orbit 20071015.hgt 20071015.ph_sim 0 0 - -  
A20071015.rslc.par
```

By specifying the ISP SLC parameter files for both images we tell the program to take into account that the two images have different carrier frequencies when generating the simulated fringes.

The generation of the differential interferogram requires the availability of a DIFF&GEO parameter file. This is generate with the program ***create_diff_par***. If a DIFF parameter already exists it should be deleted first.

```
create_diff_par 20071015_A20071015.off - 20071015_A20071015.diff_par 0
```

We can now remove the simulated phase (*.ph_sim) from the interferogram (*.int) to obtain a first version of the differential interferogram (*.diff0) using the program ***sub_phase***:

```
sub_phase 20071015_A20071015.int 20071015.ph_sim  
20071015_A20071015.diff_par 20071015_A20071015.diff0 1 0
```

The initial differential interferogram can be displayed with the intensity image in the background using the DISP program ***dismph_pwr24*** or saved to a SUNraster/bmp file with the program ***rasmph_pwr24*** and then viewed with the program ***disras***.

```
dismph_pwr24 20071015_A20071015.diff0 20071015.rml 750
```

Figure 5 illustrates the differential interferogram with the intensity image of ERS-2 in the background. The differential interferogram shows clear fringes for a large part of the area, basically everywhere where topography is flat. Total decorrelation occurs over hilly terrain where phase is pure noise. The interferogram shows residual systematic fringes, which are due to the inaccuracies in the baseline estimate from the orbits as well as on the baseline model used. These fringes need to be corrected for in a refinement step in order to obtain the true differential interferometric phase.

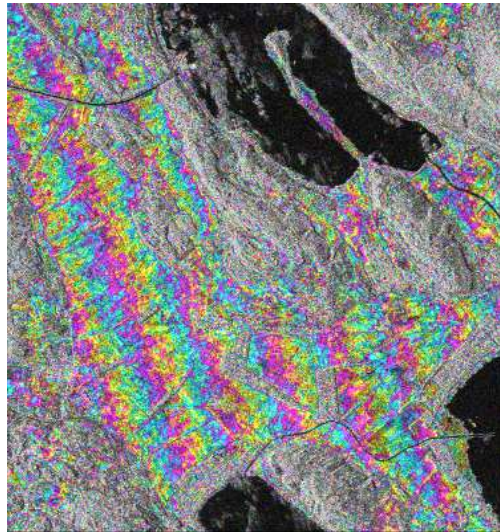


Figure 5. Initial version of differential interferogram obtained after removing from the original interferogram the curved Earth and topographic phase components based on the initial baseline estimate.

9.3. Removal of residual fringes from differential interferogram using fringe rate

To improve the differential interferogram basically we need to improve the baseline estimate. Because of the rather clear fringe pattern we can estimate the residual baseline not accounted in the initial baseline estimate from the orbits using the fringe rate and then add the residual baseline to the initial estimate to obtain an improved version of the baseline.

To determine the residual baseline using the fringe rate we use the program **base_init**. The residual baseline will be saved to the file *.base:

```
base_init 20071015.rslc.par A20071015.rslc.par 20071015_A20071015.off  
20071015_A20071015.diff0 20071015_A20071015.base 4 512 512
```

The estimated baseline perpendicular component (m) is estimated to be -14.1240 m with a rate of 0.0895 m/s, which shows that the correction to be applied is not negligible.

The initial and the residual estimate are then summed together with the program **base_add**. The file *.base1 will contain the refined estimate of the baseline.

```
base_add 20071015_A20071015.base.orbit 20071015_A20071015.base  
20071015_A20071015.base1 1
```

With the refined version of the baseline we re-simulate the curved Earth and topographic phase with the program **phase_sim**:

```
phase_sim 20071015.rslc.par 20071015_A20071015.off 20071015_A20071015.base1  
20071015.hgt 20071015.ph_sim 0 0 -- A20071015.rslc.par
```

By specifying the ISP SLC parameter files for both images we tell the program to take into account that the two images have different carrier frequencies when generating the simulated fringes.

The new simulated phase is subtracted from the original interferogram to obtain the improved version of the differential interferogram (*.diff).

```
sub_phase 20071015_A20071015.int 20071015.ph_sim  
20071015_A20071015.diff_par 20071015_A20071015.diff 1 0
```

This new differential interferogram can be displayed with the intensity image in the background just as described in Section 9.2 using the DISP program **dismph_pwr24** or saving it to a SUNraster/bmp file with the program **rasmph_pwr24**, which can then viewed with the program **disras**.

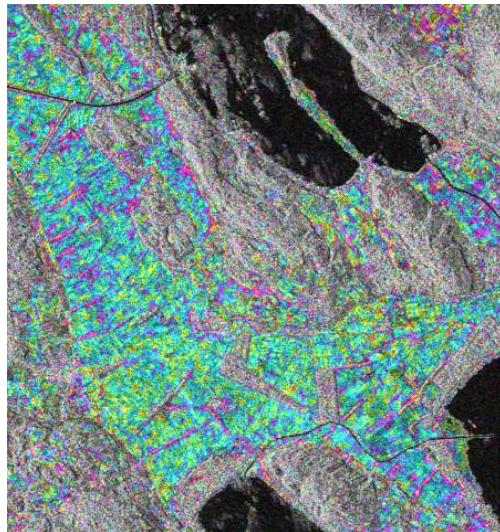


Figure 6. Differential interferogram with intensity image in the background after baseline correction.

Figure 6 illustrates the new differential interferogram with the intensity image of ERS-2 in the background. The systematic fringe pattern has apparently disappeared and the differential phase is now clearly visible. The differential phase consists primarily in this case of elevation not represented in the reference DEM. Still a light systematic phase seems to be present. In Section 9.6 we show how this can be dealt with. This differential interferogram is however sufficiently good for estimating the coherence since the systematic phase variations are of such low frequency that they practically will not affect the estimate of the coherence because of the relatively small window size used for estimating the coherence.

9.4. Generation of coherence image

With the differential interferogram we can now compute the coherence image. For this we use the program **cc_wave**. As trade-off between accurate estimation of the coherence and loss of resolution the coherence is estimated in a 5x5 window and a triangular weighting function is applied. As alternative the LAT program **cc_ad** could be used. It is referred to the ISP User's Guide for a description of the two programs.

```
cc_wave      20071015_A20071015.diff      20071015.rmli      A20071015.rmli
20071015_A20071015.cc 750 5 5 1
```

The coherence image *.cc can be displayed with the DISP program **discc**, with or without the intensity image in the background. A SUNraster/bmp version can be generated with the program **rascc** and viewed with the program **disras**.

```
discc 20071015_A20071015.cc - 750
```

Figure 7 illustrates the coherence image in grayscale. High coherence is found for most agricultural areas, which are bare around the time of the year when the image was acquired. The dark patches within the agricultural areas correspond to forest stands, which are totally decorrelated. Total decorrelation can also be seen in the top right part. This is due to the hilly topography. Comparing Figures 6 and 7 we can see that high-coherence areas present clear interferometric phase whereas low-coherence areas are characterized by noisy phase values.



Figure 7. Coherence image of the Seeland region. Bright areas correspond to high coherence (0.7-0.8), dark areas correspond to low coherence (< 0.2).

9.5. Phase unwrapping

The next step in processing consists of unwrapping the differential interferogram. This is done either if the interferogram obtained in Section 9.3 is the final version or if a refinement of it is needed.

Figure 7 shows that large part of the image has high coherence, which implies that phase unwrapping will not be extremely complicated. However, there are a few areas of high coherence that are isolated or divided by low coherence strips, which might introduce errors in the unwrapped interferogram in form of 2π jumps. A method to cope with such situation consists of unwrapping a multi-looked version of the differential interferogram. By multi-looking the interferogram we reduce the number of cases where small low-coherence strips cut areas of high coherence and obtain a more continuous area to be unwrapped. This makes phase unwrapping more reliable. The unwrapped multi-looked interferogram can then be oversampled to the original pixel size.

At first we multi-look the differential interferogram and the ERS-2 MLI image with factors 10 and 10. For this the program ***multi_cpx*** (for complex data) and ***multi_real*** (for real data) are used. The programs also generate (or update) an ISP offset parameter file that contains the parameters relative to the multi-looked images.

```
multi_cpx           20071015_A20071015.diff           20071015_A20071015.off
20071015_A20071015.diff10 20071015_A20071015.off10 10 10 0 0

multi_real          20071015.rmlri      20071015_A20071015.off           20071015.rmli10
20071015_A20071015.off10 10 10 0 0
```

To indicate that these MLIs have been obtained with multi-look factors 10 and 10 the string “10” has been added to the extension of the corresponding files. The *.diff10 and *.rmli10 files are 75 pixels wide and 80 pixels long.

Then we generate with ***cc_wave*** a multi-look coherence image (*.diff10.cc) of similar size to the multi-looked images generated above. Since this coherence image is needed to set which pixels will be unwrapped, the estimate of the coherence can be based on phase information only. From the coherence image the phase unwrapping mask is obtained with the program ***rascc_mask*** using 0.7 as threshold for the coherence. The threshold can be set by the user by looking at the multi-looked coherence image. Here we use a rather high threshold in order to be sure to unwrap only areas with reliable phase information. We will see further down in the processing, when working on a refinement level, that lower thresholds will be used.

```
cc_wave 20071015_A20071015.diff10 -- 20071015_A20071015.diff10.cc 75 7 7 1
rascc_mask 20071015_A20071015.diff10.cc - 75 1 1 0 1 1 0.7
```

We then unwrap the multi-looked differential interferogram (*.diff10) using the MCF algorithm. For more information about this phase unwrapping approach it is referred to the ISP User’s Guide.

```
mcf           20071015_A20071015.diff10           20071015_A20071015.diff10.cc
20071015_A20071015.diff10.cc_mask.ras 20071015_A20071015.diff10.unw 75 1 0
0 -- 1 1
```

The unwrapped multi-looked differential interferogram (*.diff10.unw) can be displayed with the DISP program **disdt_pwr24** with the intensity image in the background. Another way to display this image is to use the DISP program **disrimg** as shown in the ISP User's Guide.

```
disdt_pwr24 20071015_A20071015.diff10.unw 20071015.rml10 75 1 1 0 12.6 1.  
.4 1
```

Finally this unwrapped interferogram is oversampled with factors 10 and 10 to obtain the unwrapped differential interferogram in the original resolution. This is done with the program **multi_real** (the unwrapped interferogram is a real-valued image) using multi-look factors -10 and -10.

```
multi_real      20071015_A20071015.diff10.unw      20071015_A20071015.off10  
20071015_A20071015.diff.unw 20071015_A20071015.off -10 -10 0 0
```

The unwrapped differential interferogram (*.diff.unw) can be displayed with the DISP program **disdt_pwr24** with the intensity image in the background. Another way to display this image is to use the DISP program **disrimg** as shown in the ISP User's Guide.

```
disdt_pwr24 20071015_A20071015.diff.unw 20071015.rml1 750 1 1 0 12.6 1. .4  
1
```

Figure 8 shows the unwrapped differential interferogram with a color cycle of 4π . The intensity image has been used as background. The rather large color cycle has been used to detect visually possible inconsistencies in the unwrapped phases (i.e. 2π jumps). This does not seem to be the case. The “box-effect” with vertical and horizontal borders is due to the strong oversampling applied.

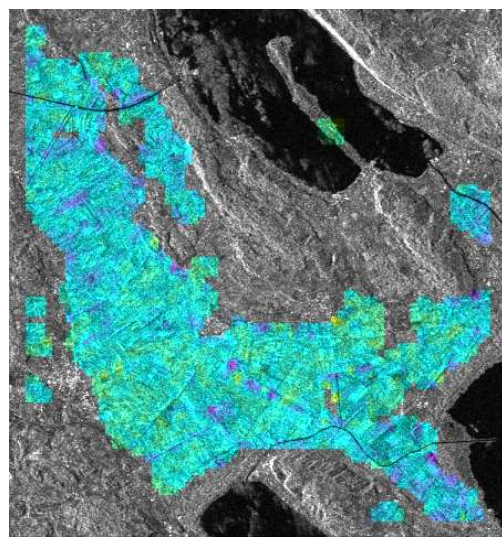


Figure 8. Unwrapped differential interferogram with a 4π color cycle.

9.6. First refinement of differential interferogram using baseline model

The differential interferogram might still have some phase trends related to an imperfect estimate of the baseline. As mentioned in the User's Guide of the ISP, the most accurate method to determine the baseline is to use ground control points (GCPs) and a baseline model. It is referred to the ISP User's Guide for more information.

Estimation of the baseline based on GCPs requires an unwrapped interferogram and a DEM in radar geometry. Since the DEM is already available, we just need to obtain an unwrapped interferogram. This can be obtained by adding the unwrapped differential phase (*.diff.unw) to the unwrapped simulated phase created in Section 9.3 (*.ph_sim). In this way we generate an unwrapped version of the original interferogram (*.int.unw). The addition of the interferograms is done with the program **sub_phase**. The resulting interferogram represents the original interferogram however with the baseline as estimates so far from orbits and fringe rate. In other words, if this baseline is not the true baseline the interferogram will contain residual systematic fringes that will be estimated with the baseline model.

```
sub_phase           20071015_A20071015.diff.unw      20071015.ph_sim
20071015_A20071015.diff_par 20071015_A20071015.int.unw 0 1
```

In order to avoid that the baseline is determined based on GCPs with low coherence, i.e. unreliable phase values, we generate a coherence image from which a mask will be obtained by using a simple threshold. The coherence image can be generated based only on the phase information in the differential interferogram since we are interested in the coherence image just as a flag. While for phase unwrapping the threshold needed to be set to a high value to avoid introducing errors in this critical first version of the unwrapped phase, for the baseline estimation we can set the threshold to a lower value, e.g. 0.4. Baseline estimation will make use of least-squares techniques so it is preferred to work with more samples, even if some are somewhat noisy, rather than with few good samples.

```
cc_wave 20071015_A20071015.diff -- 20071015_A20071015.diff.cc 750 7 7 1
rascc_mask 20071015_A20071015.diff.cc - 750 1 1 0 1 1 .4
```

To select GCPs the program **extract_gcp** is used. The GCPs are selected using the coherence mask to indicate whether a candidate point has sufficiently high coherence, i.e. sufficiently reliable phase information. The user can select the number of GCP points in range and azimuth, which are set in this example to 100 in each direction to obtain a dense net of GCPs. If the user prefers selecting GCPs manually, it is referred to the procedure described in the Examples Section of the ISP User's Guide.

```
extract_gcp 20071015.hgt 20071015_A20071015.off 20071015_A20071015.gcp 100
100 20071015_A20071015.diff.cc_mask.ras
```

The GCPs are stored in the text file *.gcp which contains the range and azimuth position of the points and the corresponding elevation. The file can be viewed with a text editor.

With the program **gcp_phase** we can now extract phase values for the selected GCPs. The elevation data and the extracted unwrapped phases are saved to the file *.gcp_ph. This is a text file that can be viewed with a text editor. To limit noise effects on the phase estimates at the GCPs position a window size of 3 pixels centered in the GCP has been selected for averaging phase.

```
gcp_phase           20071015_A20071015.int.unw      20071015_A20071015.off
20071015_A20071015.gcp 20071015_A20071015.gcp_ph 3
```

Using the phase estimates and the height values at the GCPs, a new baseline estimate is determined with the program **base_ls**. For more information on this approach it is referred to the ISP User's Guide. Before proceeding it is recommended to rename the previous baseline file in order to avoid confusion in the file names.

```
cp 20071015_A20071015.base1 20071015_A20071015.base.orig  
base_ls 20071015.rslc.par 20071015_A20071015.off 20071015_A20071015.gcp_ph  
20071015_A20071015.base1 0 1 1 1 1 1. A20071015.rslc.par
```

By specifying the ISP SLC parameter files for both images we tell the program to take into account that the two images have different carrier frequencies when generating the baseline estimate.

The previous and the new baseline estimates can be compared by opening the files *.base_orig and *.base1 with a text editor. The perpendicular and parallel components of the baseline can be viewed with the program **base_perp**. The difference between the estimates is about 0.2 m for the perpendicular component. The validity of the baseline model is certified by the low RMS altitude error (1.06 m). This value corresponds to the mean difference between the true elevation and the elevation estimated through the baseline model at the GCPs.

With this new version of the baseline we can once again generate a simulated phase image of the curved Earth and topographic components (unwrapped), which we then subtract from the original interferogram to obtain a new version of the differential interferogram.

```
phase_sim 20071015.rslc.par 20071015_A20071015.off 20071015_A20071015.base1  
20071015.hgt 20071015.ph_sim 0 1 - - A20071015.rslc.par  
  
sub_phase 20071015_A20071015.int 20071015.ph_sim  
20071015_A20071015.diff_par 20071015_A20071015.diff 1 0
```

The differential interferogram *.diff can be displayed as already described in Section 9.2. Figure 9 shows a comparison between the differential interferogram obtained from refined baselines using the fringe rate and the differential interferogram obtained from the baseline model and the unwrapped phase values. The new differential interferogram seems to present slightly less spatial variations compared to the previous version.

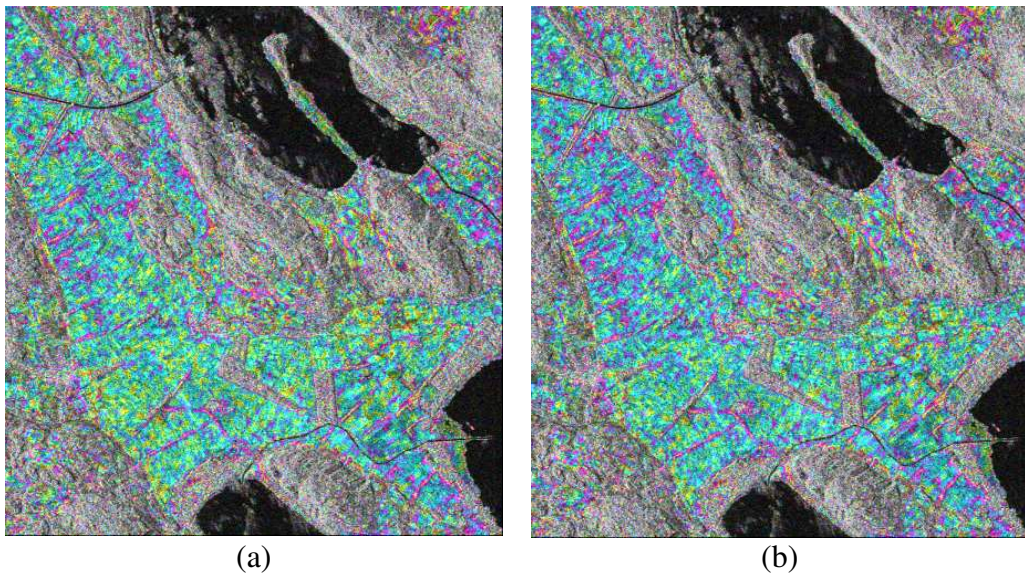


Figure 9. Differential interferogram before using baseline refinement with base_ls (a) and after using base_ls (b). The image in (a) corresponds to Figure 8.

9.7. Phase unwrapping of refined differential interferogram

Phase unwrapping of the refined differential interferogram consists of the same steps presented in Section 9.5. Therefore here only the commands are reported. Previously generated files are overwritten.

Generation of 10x10 multi-looked images of the differential interferogram and the reference MLI:

```
multi_cpx      20071015_A20071015.diff      20071015_A20071015.off
20071015_A20071015.diff10 20071015_A20071015.off10 10 10 0 0

multi_real     20071015.rmlri    20071015_A20071015.off      20071015.rmlri10
20071015_A20071015.off10 10 10 0 0
```

Generation of phase unwrapping mask

```
cc_wave 20071015_A20071015.diff10 -- 20071015_A20071015.diff10.cc 75 7 7 1
rascc_mask 20071015_A20071015.diff10.cc - 75 1 1 0 1 1 0.7
```

Phase unwrapping of multi-looked differential interferogram using MCF algorithm

```
mcf      20071015_A20071015.diff10      20071015_A20071015.diff10.cc
20071015_A20071015.diff10.cc_mask.ras 20071015_A20071015.diff10.unw 75 1 0
0 - - 1 1
```

Oversampling of unwrapped differential interferogram to original pixel size

```
multi_real     20071015_A20071015.diff10.unw      20071015_A20071015.off10
20071015_A20071015.diff.unw 20071015_A20071015.off -10 -10 0 0
```

The new unwrapped differential interferogram *.diff.unw can be displayed as already described in Section 9.5. Figure 10 shows a comparison between the previous unwrapped differential interferogram and the new version. The new differential interferogram seems to present slightly less spatial variations compared to the previous version.

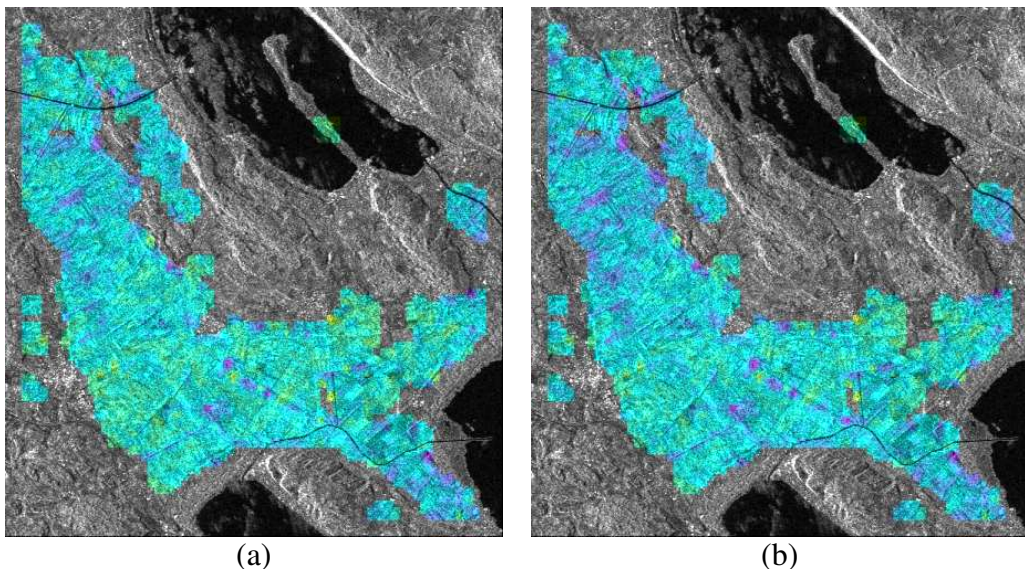


Figure 10. Unwrapped differential interferogram before using baseline refinement with base_ls (a) and after using base_ls (b). A color cycle of 4π has been applied in both cases. The image in (a) corresponds to the image in Figure 8.

9.8. Compensation of unwrapped interferogram for residual quadratic phase

It is possible that the differential interferogram still presents some residual phase components not yet compensated for after baseline improvement. This is for example the case for large baseline changes along-track due to squinted orbits. This Section deals with the correction of such quadratic phase components. This compensation requires the availability of the unwrapped differential interferogram.

At first we determine a coherence image from the differential interferogram from which we generate a mask. The mask is generated with a threshold of 0.35. With respect to previously computed coherence images here we use a very large window (15x15) to be sure that low coherence pixels are excluded from the estimation of the quadratic phase component. To avoid losing too much resolution Gaussian windowing is applied.

```
cc_wave 20071015_A20071015.diff -- 20071015_A20071015.cc2 750 15 15 2  
rascc_mask 20071015_A20071015.cc2 - 750 1 1 0 1 1 .35
```

The mask is then applied to determine the model phase function. This requires the unwrapped version of the differential interferogram to be corrected. For this we use the program **quad_fit** with default values, with masking for low coherence pixels and assuming a quadratic phase model as follows:

```
quad_fit 20071015_A20071015.diff.unw 20071015_A20071015.diff_par 32 32  
20071015_A20071015.cc2_mask.ras quad_fit.plot 0
```

The phase model is saved to the *.diff_par file. The phase fit at the points selected in the interferogram is saved to the text file quad_fit.plot, which can be displayed e.g. with the program xmgrace. The report of the processing indicates that a non-zero model was fitted to the observations. The error statistics in form of standard deviation of the phase fit is 0.5804 radians.

The model fit is now applied to the differential interferogram with the program **quad_sub** to obtain a refined version of it, called *diff2.unw.

```
quad_sub 20071015_A20071015.diff.unw 20071015_A20071015.diff_par  
20071015_A20071015.diff2.unw 0 0
```

This new unwrapped differential interferogram *.diff2.unw can be displayed as already described in Section 9.5. Figure 11 shows a comparison between the previous unwrapped differential interferogram and this new version. A further improvement can be noticed since the phase has become slightly more homogeneous (more bluish tones) especially in the central part of the image.

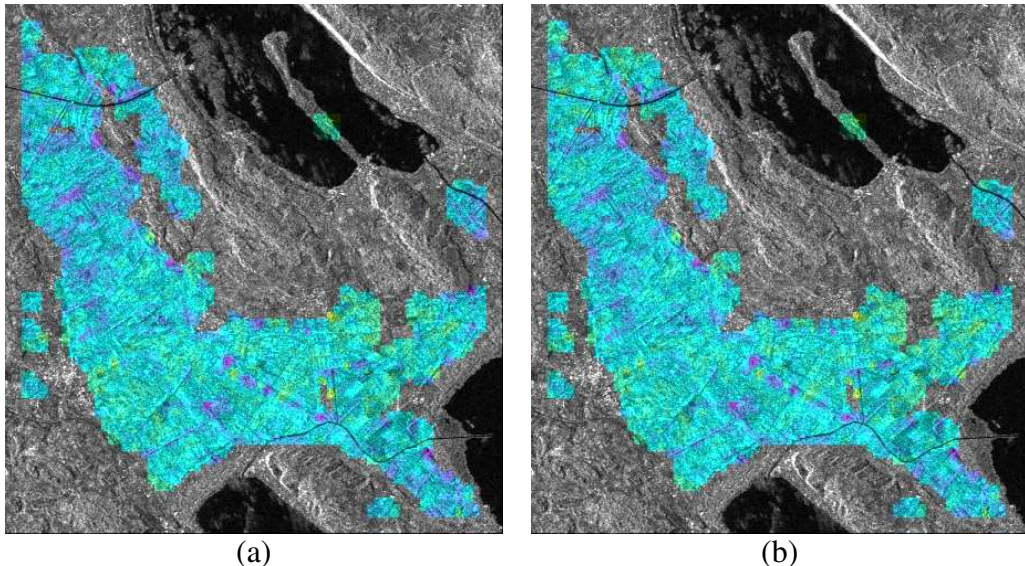


Figure 11. Unwrapped differential interferogram before correcting for quadratic phase terms (a) and after the correction (b). A color cycle of 4π has been applied in both cases. The image in (a) corresponds to the image in Figure 10b.

9.8. Refinement of the differential interferogram with improved quadratic phase model

It is possible that the model used for the compensation of quadratic phase terms might include a certain error in case there have been errors in the phase unwrapping stage before estimating the quadratic phase model. To avoid that possible unwrapping errors propagate to the final result, a possibility is to use the quad_fit-based estimate, remove it from the wrapped differential interferogram obtained in Section 9.6 (the one obtained after the baseline correction with **base_ls**), unwrap this further refined differential interferogram, re-estimate the quadratic phase term and remove it from the unwrapped interferogram.

Let us first rename to the *.diff interferogram to *.diff0 to avoid complications with file names further down in the processing. As a matter of fact the extension “diff” is meant to be used for sort of output differential interferograms whereas “diff0” is used for differential interferograms to be substantially refined.

At first the estimate of the quadratic phase trend obtained in Section 9.7 is subtracted from the differential interferogram (*.diff0) to obtain a new version of the wrapped differential interferogram (*.diff):

```
quad_sub          20071015_A20071015.diff0          20071015_A20071015.diff_par
20071015_A20071015.diff 1 0
```

Then we unwrap this corrected differential interferogram using the phase unwrapping procedure described in Section 9.5.

At first we generate a multi-looked version of this differential interferogram. The previous version is overwritten.

```
multi_cpx          20071015_A20071015.diff          20071015_A20071015.off
20071015_A20071015.diff10 20071015_A20071015.off10 10 10 0 0
```

We then smooth the multi-looked interferogram by applying the adaptive filter implemented in the program **adf**. In this way we improve the quality of the differential fringes.

```
adf      20071015_A20071015.diff10      20071015_A20071015.diff10.sm1  
20071015_A20071015.diff10.sm.cc 75 0.25 8 7 1 0 0 0.2
```

```
adf      20071015_A20071015.diff10.sm1      20071015_A20071015.diff10.sm2  
20071015_A20071015.diff10.sm.cc 75 0.25 8 7 1 0 0 0.2
```

The smoothed multi-looked interferogram (*.diff10.sm2) can be displayed with the DISP program **dismph_pwr24** as follows:

```
dismph_pwr24 20071015_A20071015.diff10.sm2 ave.rml10 75 1 1 0 1 .4 1
```

For phase unwrapping we want to use a mask to leave out pixels with low coherence. In Section 9.5 we generated a multi-looked coherence image (*.diff10.cc) and from it we obtained a mask using a high threshold (0.7). Now that we are working with a better version of the differential interferogram, which has also been filtered, we can relax a bit on the threshold and generate from the same multi-looked coherence image another mask. The selected threshold is 0.5, which is based on an observation of the coherence image. With a lower threshold we increase the area that is being unwrapped. The command to generate the new unwrapping mask is the following.

```
rascc_mask 20071015_A20071015.diff10.cc - 75 1 1 0 1 1 0.5
```

We can now proceed with unwrapping the smoothed multi-looked differential interferogram:

```
mcf      20071015_A20071015.diff10.sm2      20071015_A20071015.diff10.cc  
20071015_A20071015.diff10.cc_mask.ras 20071015_A20071015.diff10.unw 75 1 0  
0 - - 1 1
```

The unwrapped multi-looked differential interferogram (*.diff10.unw) can be displayed with the DISP program **disdt_pwr24** with the intensity image in the background. Another way to display this image is to use the DISP program **disrmg** as shown in the ISP User's Guide.

```
disdt_pwr24 20071015_A20071015.diff10.unw 20071015.rml10 75 1 1 0 12.6 1.  
.4 1
```

A further improvement of this unwrapped interferogram can consist of interpolating the phase values over (small) areas where no unwrapping took place to obtain a more continuous pattern of the unwrapped interferogram. This can be done with the program **interp_ad** as follows:

```
interp_ad 20071015_A20071015.diff10.unw 20071015_A20071015.diff10.unw1 75 1  
4 128 2 2 0
```

The original and the interpolated unwrapped interferograms can be displayed simultaneously with the DISP program **dis2rmg**. The interpolated interferogram presents a clearer continuity.

```
dis2rmg 20071015_A20071015.diff10.unw 20071015_A20071015.diff10.unw1 75 75  
1 1000 0 0 1.
```

We can now resample the interpolated, unwrapped multi-looked interferogram to the original size.

```
multi_real      20071015_A20071015.diff10.unw1      20071015_A20071015.off10  
20071015_A20071015.diff.unw 20071015_A20071015.off -10 -10 0 0
```

The new unwrapped differential interferogram *.diff.unw can be displayed as already described in Section 9.5. Figure 12 shows a comparison between the previous unwrapped differential interferogram obtained after removing the first estimate of the quadratic phase term and the new unwrapped differential interferogram. This differential interferogram covers now a larger area, is smoother and appears somewhat more homogeneous.

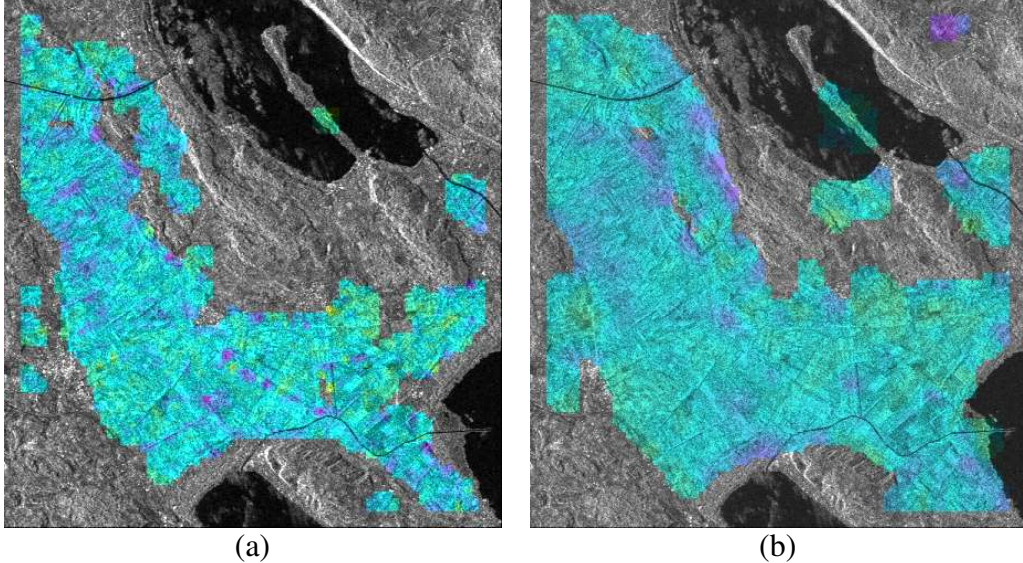


Figure 12. Unwrapped differential interferogram before refining for quadratic phase terms (a) and after the correction (b). A color cycle of 4π has been applied in both cases. The image in (a) corresponds to the image in Figure 11b.

We add now the quadratic phase model to the unwrapped interferogram in order to obtain an unwrapped interferogram of the same type the one at the end of Section 9.7, i.e. after compensation of baseline effects with base_ls, but now with in theory less errors due to phase unwrapping. This is done in order to obtain an improved interferogram in terms of phase unwrapping with respect to the one obtained after base_ls.

```
quad_sub      20071015_A20071015.diff.unw      20071015_A20071015.diff_par
20071015_A20071015.diff3.unw 0 1
```

From this improved unwrapped interferogram we re-estimate the quadratic phase term and subtract this refined quadratic phase model to obtain a new unwrapped differential interferogram compensated for the refined quadratic phase terms, just as described in Section 9.8. In theory the error statistics of the fit should now decrease since we are working with an interferogram that should have less unwrapping errors than the one used for the first fit.

```
quad_fit 20071015_A20071015.diff3.unw 20071015_A20071015.diff_par 32 32
20071015_A20071015.cc2_mask.ras quad_fit.plot 0
```

```
quad_sub      20071015_A20071015.diff3.unw      20071015_A20071015.diff_par
20071015_A20071015.diff.unw 0 0
```

Compared to the first compensation for quadratic phase the standard deviation of SVD phase fit obtained from quad_fit has decreased to 0.4988 indicating a slight improvement of the model fit.

The new unwrapped differential interferogram *.diff.unw can be displayed as already described in Section 9.5. Figure 13 shows a comparison between the previous unwrapped differential interferogram obtained after removal of the quadratic phase term and the newly

unwrapped version of it taking into account a refinement of the phase unwrapping based on the quadratic phase model. The two unwrapped interferograms are very similar, thus showing that the unwrapping was already good.

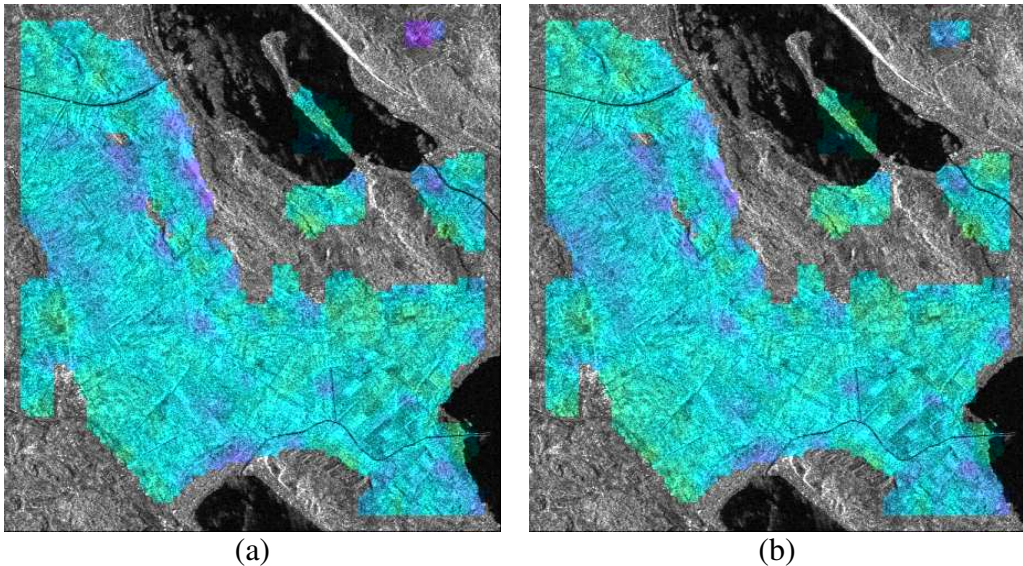


Figure 13. Unwrapped differential interferogram before refining the unwrapping with quadratic phase terms (a) and after (b). A color cycle of 4π has been applied in both cases. The image in (a) corresponds to the image in Figure 12b.

9.9. Further possible refinements and final phase unwrapping

So far we did not consider errors related to the DEM nor we considered atmospheric components to be present. Such kind of errors can influence several aspects of the interferometric processing such as the phase simulation, the phase unwrapping stage, the refinement of the baseline with base_ls etc. One way to deal with this situation is to exclude areas where known errors are occurring. Masking for example the DEM for specific height levels and applying the mask in the phase unwrapping will avoid that phase in the areas excluded in the mask will affect the results.

Assuming that the interferogram obtained with the first iteration of **quad_fit** is unwrapped sufficiently well, we can proceed with the inversion to height.

At first we can obtain the final version of the unwrapped differential interferogram using the *.diff.unw file from the last Section as model for the unwrapped phase. The idea is that the unwrapped differential interferogram represents a model for the final unwrapped phase in the sense that we assume that this unwrapped phase is in the same $(-\pi, +\pi)$ interval of the true phase and that it can be used to obtain this true phase from the interferogram to be unwrapped. This is done with the program **unw_model** (see also ISP User's Guide). After completion of the unwrapping a phase constant is subtracted from all unwrapped phase values such that the unwrapped phase at the indicated reference location (200,500) will correspond to the indicated reference phase value (0.0 in the example).

```
unw_model          20071015_A20071015.diff          20071015_A20071015.diff.unw
20071015_A20071015.diff.unw2 750 200 500 -
```

9.10. Conversion of unwrapped phase to elevation

The final differential interferogram contains only residual heights with respect to the reference DEM. This could be therefore used for example for comparing DEMs. It is however more interesting to add the unwrapped phase to the simulated phase based on the DEM and invert this to height.

To add the unwrapped differential interferogram (*.diff.unw2) to the simulated phase (*.ph_sim) we use the program **sub_phase** in order to obtain the unwrapped interferogram *.int.unw2.

```
sub_phase           20071015_A20071015.diff.unw2           20071015.ph_sim
20071015_A20071015.diff_par 20071015_A20071015.int.unw2 0 1
```

This is then converted to height with the program **hgt_map**. The output consists of the InSAR DEM *.hgt2 and the ground ranges map *.grd2.

```
hgt_map           20071015_A20071015.int.unw2           20071015.rslc.par
20071015_A20071015.off 20071015_A20071015.base1 20071015.hgt2 20071015.grd2
0 0 - A20071015.rslc.par
```

The original DEM and this interferometric DEM can be displayed for example simultaneously with the program **dis2hgt**:

```
dis2hgt 20071015.hgt2 20071015.hgt 750 750 - - - 7
```

In Figure 14 we illustrate the original DEM and the ERS-ENVISAT DEM with a color cycle of 7 meters. The two DEMs show the same elevation pattern. The ERS-ENVISAT DEM shows finer details because of the better resolution compared to the SRTM-3 DEM and the strong sensitivity to elevation variations. Striking are the worm-like structures corresponding to old riverbeds with an elevation difference of 1-2 m. The disadvantage of the ERS-ENVISAT DEM is the coverage. Areas with strong topography have been masked out during processing because of the strong decorrelation.

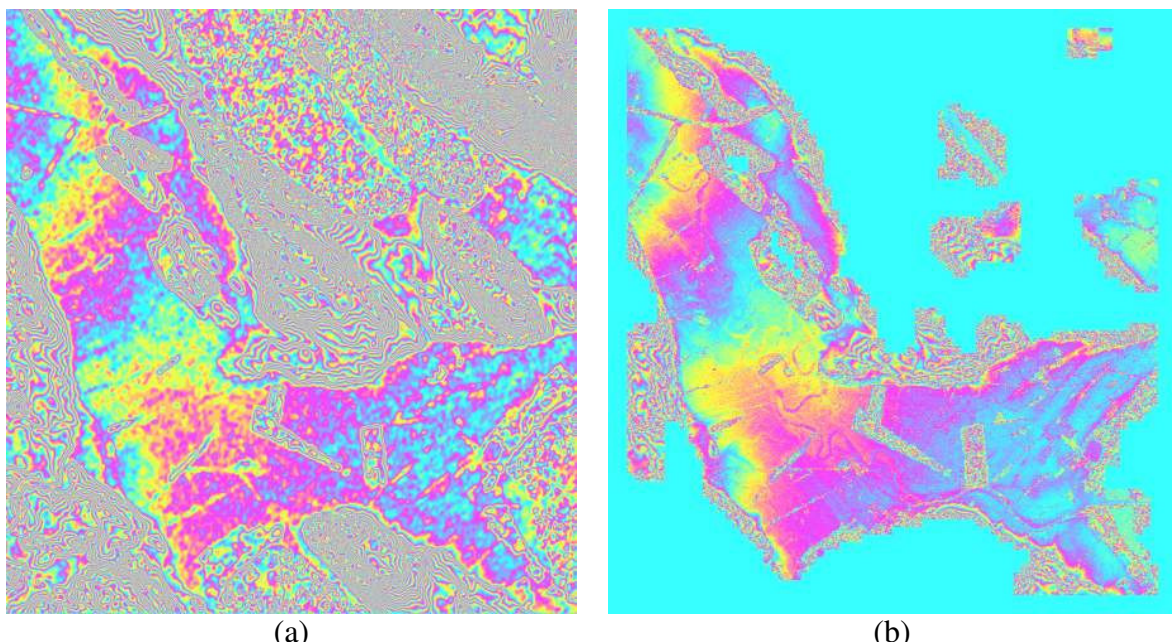


Figure 14. Reference SRTM-3 DEM (a), ERS-ENVISAT DEM (b) for the Seeland region. A color cycle of corresponds to 7 m elevation difference. For areas on hilly terrain no elevation has been retrieved in (b).

10. References

- [1] M. Santoro, J. I. H. Askne, U. Wegmüller, and C. L. Werner, "Observations, modeling, and applications of ERS-ENVISAT coherence over land surfaces," IEEE Trans. Geosci. Remote Sensing, vol. 45, pp. 2600-2611, 2007.
- [2] U. Wegmüller, M. Santoro, C. Werner, T. Strozzi, A. Wiesmann, W. Lengert, and N. Miranda, "ERS-2 Zero-Gyro-Mode data application showcases," Proc. Fringe 2007 Workshop, ESA-ESRIN, Frascati, 26-30 November, 2007.